Facilitated Lewis Acid Transfer by Phospholipids at a (Water|CHCl3) Liquid|Liquid Interface toward Biomimetic and Energy Applications

T. Jane Stockmann, Jean-Marc Noël, Ali Abou-Hassan, Catherine Combellas, Frédéric Kanoufi

Facilitated Lewis Acid Transfer by Phospholipids at a (Water|$CHCl_3$) Liquid|Liquid Interface Toward Biomimetic and Energy Applications

T. Jane Stockmann,[a] *Jean-Marc Noël,*[a] *Ali Abou-Hassan,*[b] *Catherine Combellas,*[a] *and Frédéric Kanoufi*[a,*]

[a] Sorbonne Paris Cité, Paris Diderot University, Interfaces, Traitements, Organisation et Dynamique des Systèmes, CNRS-UMR 7086, 15 rue J. A. Baif, 75013 Paris - France.

[b] Sorbonne Universités, UPMC Univ Paris 06, Physico-chimie des Electrolytes, Nanosystèmes Interfaciaux (PHENIX), CNRS-UMR 823, 4 place Jussieu, F-75005, Paris, France

AUTHOR INFORMATION

Corresponding Author

*Tel.: +33 (0)1 57 27 72 17; Fax: +33 (0) 1 57 27 72 63; E-mail address: frederic.kanoufi@univ-paris-diderot.fr; URL: http://www.itodys.univ-paris7.fr/ (F. Kanoufi)

ABSTRACT. Proton and metal ion interaction with phospholipids are of considerable interest to biological applications (*e.g.* chemical communication, drug transport, etc.). Herein, H^+ and Li^+ coordination to a typical phospholipid are examined electrochemically at the water|chloroform micro-interface, which reveals two coordination stoichiometries towards protons that were

thermodynamically quantified using cyclic voltammetry. The thermodynamics of phospholipid facilitated proton transfer are further confirmed through Comsol Multiphysics simulations. Insight into H^+-phospholipid coordination/interaction has valuable implications towards cellular communication (such as vesicle systems that mimic living cells) and vesicle micro-reactor synthetic applications; however, the utility of the H^+/phospholipid coupled water|organic solvent system is exemplified herein towards the batch generation of solar fuels through shake-flask experiments.

INTRODUCTION

Many cellular processes, such as those involved in the cell energy machinery, depend on the transport of ions across phospholipidic biological membranes. An illustration is the transfer of protons to generate ATP involved in cellular respiration. In addition to the well-known role of proton pumps (or ion channels), recent experiments[1] and molecular dynamics simulations[2] suggest that the phospholipid itself, even devoid of protonable moieties, presents a high proton affinity, ensuring a high H^+ concentration at the water/phospholipid interface. In principle this concept can be generalized to alkali metal ions and to biomimetic analogs of living cells such as vesicles or simple/double emulsion systems employing phospholipids. These artificial cell-like platforms are largely employed in various applications and are particularly a key-ingredient for the compartmentalization of (bio)chemical information or chemical reactions in droplet-based microfluidics.[3-5]

By the encapsulation of chemical systems, vesicles become a powerful utility, particularly with respect to a generalized view of how chemical species interact with the lipid bilayer,[4-6] through their transport between vesicles. The importance of the transport (or permeability) of H^+, and that of related Lewis acids, through phospholipid layers is particularly challenged by the recent

reports on the high affinity and fast diffusion of H^+ within the lipids comprising the vesicle membrane.[1,2] For a specific understanding, it is necessary to analyze the various components in isolation: *e.g*. the specific interaction of protons with phospholipids. This can be accomplished by depositing phospholipids in mono- or bilayers at the liquid/air[7,8] and liquid|liquid interfaces[4,8-15] and electrochemically stimulating that interface with a probe or through the charge transfer of different chemical species; *e.g*. protons, particularly in the case of the latter.

Liquid|liquid electrochemistry,[16-18] at the interface between two immiscible electrolytic solutions (ITIES), offers a valuable biomimetic approach since the interface, typically between water and an organic solvent (w|o), *e.g*. water|1,2-dichloroethane (w|DCE),[19] is similar to the water|lipid biological interface. Indeed, it has been used to investigate ion transfer reactions of significant biomolecules[20-22] and understand the interaction of ions with nanopore[23-25] structures common in living cells. By functionalizing the w|o interface with phospholipids, kinetic and thermodynamic insight through direct electrochemical measurements can be gained concerning ion transfer,[26] ion adsorption,[11] or facilitated ion transfer reactions.[11,25,27-29]

However, phospholipids are difficult to analyze due to their lack of solubility in conventional liquid|liquid electrochemical solvents. They are usually dissolved in low polarity solvents, such as chloroform ($CHCl_3$, $\varepsilon = 4.81$),[30] which are often avoided owing to their high resistivity for electrochemical measurements.[31] An active area of research[32,33] consists in overcoming such limitations through the use of (i) micro-ITIES coupled with (ii) an ionic liquid (IL) as the supporting electrolyte.[31] Furthermore, by using chloroform, appreciable concentrations of 1,2-dimyristoyl-sn-glycero-3-phosphocholine (DMPC) – employed herein as a model phospholipid – could be analyzed thus improving the response signal.

Herein, we have studied by cyclic voltammetry (CV) the interaction between a Lewis acid (H^+ or Li^+) and a phospholipid (DMPC) at a w|$CHCl_3$ micro-interface. CV demonstrates that DMPC facilitates the transfer of H^+ and Li^+ across the interface; furthermore, this process is thermodynamically favourable. In order to highlight a potential application, the facilitated, catalytic transfer of H^+ has been demonstrated towards solar fuel generation (*i.e.* for O_2 reduction or H_2 evolution) through shake-flask experiments, where decamethylferrocene ($Cp^*_2Fe(II)$) was employed as a sacrificial electron donor.

EXPERIMENTAL

Reagents were obtained commercially and used as received, including lithium sulfate (Li_2SO_4, VWR, Fontenay-sous-Bois, FR), and sulfuric acid (Alfa Aesar, Ward Hill, US), while octyltriethoxysilane, tetramethylammonium bromide (TMABr), decamethylferrocene ($Cp^*_2Fe(II)$), tetradecylammonium tetrakis(para-chlorophenyl)borate (TDATPBCl), chloroform (for HPLC, ≥99.9%) and sodium tetraphenylborate (NaTPB) were bought from Sigma-Aldrich/Fluka (L'Isle d'Abeau Chesnes, FR). 1,2-dimyristoyl-sn-glycero-3-phosphocholine (DMPC) was sourced from Echelon Bioscience (Le Perray en Yvelines, France). All aqueous solutions were prepared using Milli-Q ultrapure water (≥ 18.2 MΩ·cm).

The tetraoctylphosphonium tetrakis(pentafluorophenyl)borate ionic liquid ($P_{8888}TB$) was prepared through a metathesis reaction between tetraoctylphosphonium bromide (Sigma-Aldrich) and tetrakis(pentafluorophenyl)borate lithium etherate (Boulder Scientific, Longmont, CO) in dichloromethane as described elsewhere.[34] Tetramethylammonium tetraphenylborate (TMATPB) was prepared similarly by combination of TMABr and NaTPB in a 1:1 molar ratio in water (99% yield), subsequently rinsed with water, dried, and structurally confirmed through ^{1}H-NMR

(CD_3CN, 400 MHz) δ (ppm): 3.04 (s, 12 H), 6.84 (t, 4 H), 6.99 (t, 8 H), 7.27 (m, 8 H) which agrees well with that shown previously.[35]

UV/Visible spectra were acquired using a Perkin Elmer Lambda 1050 UV/Vis/NIR Spectrometer equipped with 3D WB Detection Module (Waltham, MA).

Electrochemical measurements were recorded using a potentiostat from CH-Instruments (model#720, Austin, Texas) and the electrochemical cells illustrated in Scheme 1.

$$\mathrm{Pt}\left|\mathrm{Pt_2SO_4}\right|\begin{matrix}5\text{ mM }\mathrm{H_2SO_4}\\(w)\end{matrix}\left\|\begin{matrix}y\text{ mM DMPC}\\5\text{ mM }\mathrm{P_{8888}TB}\\(CHCl_3)\end{matrix}\right|\mathrm{PtTB}\left|\mathrm{Pt}\right. \qquad \text{[Cell 1]}$$

$$\mathrm{Pt}\left|\mathrm{Pt_2SO_4}\right|\begin{matrix}z\text{ mM }\mathrm{H_2SO_4}\\(w)\end{matrix}\left\|\begin{matrix}0.75\text{ mM DMPC}\\5\text{ mM }\mathrm{P_{8888}TB}\\(CHCl_3)\end{matrix}\right|\mathrm{PtTB}\left|\mathrm{Pt}\right. \qquad \text{[Cell 2]}$$

$$\mathrm{Pt}\left|\mathrm{Pt_2SO_4}\right|\begin{matrix}z\text{ mM }\mathrm{H_2SO_4}\\(w)\end{matrix}\left\|\begin{matrix}1.0\text{ mM DMPC}\\5\text{ mM TDATPBCl}\\(CHCl_3)\end{matrix}\right|\mathrm{PtTB}\left|\mathrm{Pt}\right. \qquad \text{[Cell 3]}$$

Scheme 1: Schematic representations of the electrolytic cells employed where the [DMPC, 1,2-dimyristoyl-sn-glycero-3-phosphocholine)] (y) was varied from 0 to 1.0 mM in Cell 1 and [H_2SO_4] (z) from 25 to 150 mM in Cells 2 and 3. Tetraoctylphosphonium tetrakis(pentafluorophenyl)borate ($P_{8888}TB$) and tetradecylammonium tetrakis(para-chlorophenyl)borate (TDATPBCl) ionic liquids were used as organic phase supporting electrolytes.

The aqueous phase was back-filled into a pulled borosilicate glass capillary (the fabrication of which has been described in detail elsewhere[27,36]). The capillary was in-turn fixed inside a modified pipette holder (HEKA Instruments, Nova Scotia),[37] and filled from the back with the

aqueous phase so that the w|$CHCl_3$ interface was positioned at the tip of the capillary using a syringe. The tip was then immersed in the $CHCl_3$ phase. The w|$CHCl_3$ interface was continuously monitored using a CCD camera attached to a 12× zoom lens assembly (Navitar, Rochester, NY). The diameter of the immiscible interface between the two electrolytic solutions (ITIES) was determined to be 25 μm via an optical microscope. The potential scale was referenced relative to the ion transfer potential of tetramethylammonium (TMA^+), 0.208 V, which was added at a concentration of 0.5 mM of TMACl to the aqueous phase. The formal ion transfer potential for TMA^+ was estimated by using the point-of-zero-charge (PZC) from a blank CV, without TMACl added, and using 5 mM Li_2SO_4 as the aqueous phase supporting electrolyte. The PZC, in turn, was taken to be the midpoint between the two polarizable potential limits at a micro-ITIES.

RESULTS AND DISCUSSION

Figure 1A illustrates the CVs obtained through Cell 1 (Scheme 1 and Figure 1B), at a scan rate of 0.020 V s^{-1} and with increasing [DMPC] (y), from 0 to 1 mM, while z was maintained at 5 mM H_2SO_4. In the blank curve (dashed black trace) the polarizable potential window (PPW) is limited at positive and negative potentials by the transfer of H^+ and SO_4^{2-} (or HSO_4^-), respectively, from w to o. After addition of 0.25 mM of DMPC to the $CHCl_3$ phase, two sigmoidal, or s-shaped, waves appear in the forward and reverse scans with half-wave potentials ($\Delta_o^w\phi_{1/2}$) between 0.000-0.050 V for the first and 0.290-0.350 V for the second wave. Meanwhile, the baseline corrected steady-state current (i_{ss}) for each wave increases linearly with [DMPC] for both waves. Since i_{ss} is positive, it can be concluded that a cation is transferring from w to o. However, because the pipette geometry is asymmetric, its CV response for simple ion transfer is also asymmetric (Figure S1 in SI); therefore, this is an organic phase diffusion limited process

and it can be concluded that DMPC is facilitating proton transfer from w to o.[17,38] Furthermore, the appearance of two curve features suggests that there are multiple proton to DMPC coordination ratios and at least two protons are exchanged.

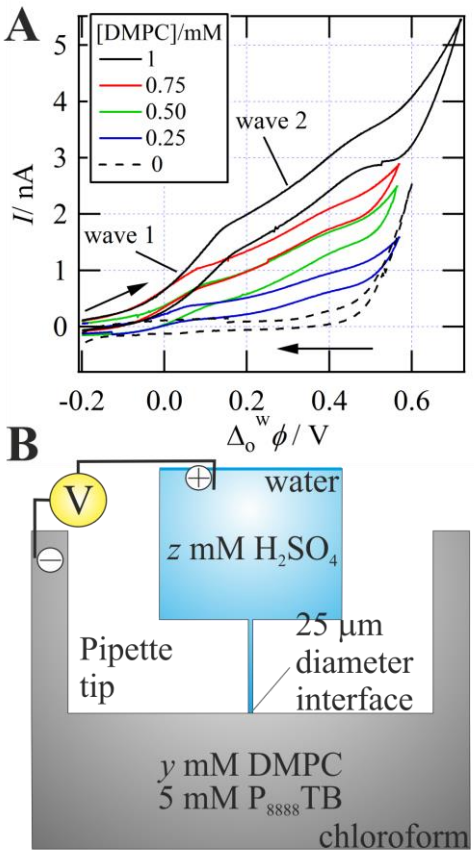

Figure 1: **A**: Cyclic voltammograms at a w|$CHCl_3$ micro-interface (25 µm diameter), using Cell 1 (see Scheme 1) illustrated in **B** for different concentrations (*y*) of DMPC. Scan rate = 0.020 V s^{-1}. **B**: Cartoon of the micropipette tip immersed in $CHCl_3$.

To further test the proton-DMPC coordination hypothesis, H_2SO_4 in Cell 1 was replaced with 5 mM of Li_2SO_4; whereby, the CVs depicted in Figure 2 (and Figure S2 in the SI) were recorded. A single steady-state wave was observed during the forward scan at low [DMPC]; however, as [DMPC] increases the transfer wave merges with the positive limit of the PPW (red trace in Figure 2 and curves c-e in Figure S2 of the SI). This indicates that Li^+ can also coordinate to

DMPC. The Galvani potential difference between the two phases, with the potential drop localized across the w|o interface ($\phi_w - \phi_o = \Delta_o^w\phi$), is the driving force for ion transfer. In these cases, a higher applied potential is indicative of more energy being required to elicit charge transfer. Based on $\Delta_o^w\phi_{1/2}$ for Li^+-DMPC and the two H^+-DMPC transfer waves, one can qualitatively estimate the coordination strength of DMPC in decreasing order as $H^+_{wave\ 1}$>Li^+≈ $H^+_{wave\ 2}$. Furthermore, owing to the i_{ss} response one can conclude that, without the use of appreciable concentrations (>100 μM) of the phospholipid in $CHCl_3$, these signals, and therefore these transfer waves, would not be observable.

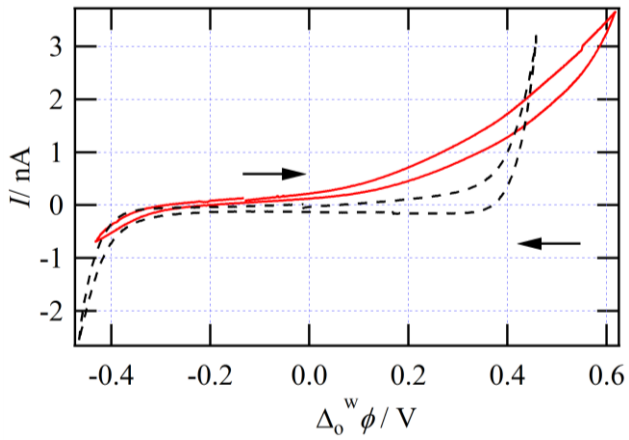

Figure 2: Cyclic voltammograms using Cell 1 where H_2SO_4 has been replaced by 5 mM Li_2SO_4, with the concentration of DMPC (*y*) varied from 0 (black dashed curve) to 0.75 mM (red trace). All other parameters are the same as those described in Figure 1. See also Figure S2 in the SI.

These results agree with recent molecular dynamics simulations of both the w|$CHCl_3$[39,40] and w|DMPC[2] interfaces. The former was shown to be highly polarized, with a dipole pointing from the water side towards the $CHCl_3$ one. This apparent positive charge on the water side explains the reported preferred physisorption of HO^- at w|o interfaces.[41] It also suggests H^+ or Li^+ are expelled from the interface, in agreement with the large overpotential required for their direct

transfer to $CHCl_3$. Moreover, simulations at the w|DMPC interface[2] evidenced a high binding affinity for H^+ and DMPC; particularly, two binding sites (the lipid's phosphate and carbonyl) and two energy minima are described. These overall simulated pictures fit with the role of DMPC facilitating H^+ (equivalently Li^+) transfer at the w|$CHCl_3$ interface.

They also favor a mechanism of facilitated ion transfer through interfacial complexation (TIC) (see Figure S3 in SI for description of possible mechanisms), summarized by:

$$m\mathrm{H}_w^+ + n\mathrm{DMPC} \rightleftharpoons [\mathrm{H}_m\text{-}\mathrm{DMPC}_n]_o^{m+} \quad (1)$$

Here, *m* and *n* are the stoichiometric coefficients of protons and DMPC, respectively.

The thermodynamics of facilitated proton transfer was further investigated by changing the acid concentration in Cell 2 while [DMPC] was maintained (y = 0.75 mM). In the resultant CVs (Figure S4), as $[H_2SO_4]$ was increased from 25 to 150 mM for curves a-e, the half-wave potential of waves 1 and 2 shifts from –0.120 to –0.260 V and 0.200 to 0.120 V, respectively. As the concentration of protons increases the applied potential (*i.e.* the amount of energy or driving force) required to elicit charge transfer decreases, in good agreement with previous reports.[27,28,42] For an acid in excess compared to DMPC, the half-wave potential of the complex ($\Delta_o^w\phi_{1/2,\text{H-DMPC}}$) will shift correspondingly with the initial concentration of protons and DMPC in each phase, $c_{\mathrm{H}^+}^*$ and c_{DMPC}^*, through the following relationship, where $\Delta_o^w\phi_{\mathrm{H}^+}^{o'}$ is the formal proton transfer potential at the w|$CHCl_3$ interface (estimated to be 0.580 V based on the formal proton transfer at a w|DCE interface[43]):

(2)

R, T, z, and F have their usual thermodynamic significance. Eq. 2 is established assuming that the most abundant DMPC species near the w|o interface is the fully protonated form as depicted in (1). It provides access to the overall constant, β, of complexation, along with the ligand stoichiometry (n, m). If one assumes a value of $n = 1$, then whatever the value of m, Eq. 2 reduces to a linear relationship with one variable on the left-hand side, a slope of 1, and a y-intercept equal to lnβ:

$$-\frac{zF}{RT}\left(\Delta_o^w\phi_{1/2,\text{H-DMPC}} - \Delta_o^w\phi_{H^+}^{o'}\right) = \frac{1}{m}\ln\beta + \ln c_{H^+}^* \qquad (3)$$

The half-wave potentials measured using Cell 2 (CVs in Figure S4 of the SI) while varying [H_2SO_4] were treated using (3) and plotted in Figure 3 (red traces) versus ln[$c_{H^+}^*$]; the results of the linear regression analysis are given in Table S1 (SI). The slope for both waves is ~1. Therefore, the H-DMPC$^+$ complex is likely operating at a 1:1 ratio with H^+ coordinating in discreet events to two different sites on the DMPC molecule with varying coordination strengths. These sites likely include the phosphine oxide and carbonyl moieties with the former being the more highly coordinating, as previously demonstrated.[37,44]

In another experiment, P_{8888}TB was replaced with tetradecylammonium tetrakis(para-chlorophenyl)borate (TDATPBCl) as the $CHCl_3$ phase supporting electrolyte, while [H_2SO_4] was varied (Cell 3, Scheme 1); the CVs are plotted in Figure S5 (SI). Two DMPC facilitated proton transfer waves were again observed and the values for $\Delta_o^w\phi_{\text{H-DMPC},1/2}$ were treated using (3) (Figure 3 and Table S1 in the SI). The linear fitting of the $\Delta_o^w\phi_{\text{H-DMPC},1/2}$ shift revealed a slope for both waves of ≈ 3. The predicted variation provided in (2) shows that for excess [H^+] the slope should be 1 whatever the extent of protonation of the ligand. However, a slope larger than 1 indicates that H^+ in the water phase is no longer in excess and is substantially consumed at the

interface. The IL incorporated TB^- (tetrakis(pentafluorophenyl)borate) is known to show little interaction or ion pairing,[45] as well as being highly stable in acidic media;[46] this is not the case for $TPBCl^-$, which decomposes readily in an acidic solution(Figure S6 in SI). Furthermore, the formation of HTPBCl was observed electrochemically and with the naked eye by H^+ transfer through a phospholipid coated droplet.[11] Therefore, it is likely that $TPBCl^-$ interferes with DMPC facilitated proton transfer, artificially altering the $\Delta_o^w\phi_{H-DMPC,1/2}$ shift response – through either a coordination or decomposition mechanism. Interestingly, even if this decomposition is almost inoperative in the absence of DMPC (meaning that $TPBCl^-$ overall protonation is much less favorable than that of DMPC) it is kinetically enhanced by the facilitated DMPC-H^+ transfer.

In previous studies at large scale (cm^2) w|DCE interfaces,[10,11,47] the analysis relied on capacitance measurements with no clear ion transfer waves and only catalytic concentrations (μM) of the phospholipid. For example, Mareček *et al*. investigated the proton-phospholipid interaction using CV at a 20-26 mm^2 w|DCE interface;[47] however, they only employed a modicum (25 μM) of phospholipid and observed an adsorption wave that was resolved at moderate scan rates (0.5-3 V s^{-1}). Through a rigorous data treatment analysis, they suggested a five-part mechanism involving the adsorption of the proton and phospholipid species at the interface as well as the eventual coordination of protons to an anionic species in the organic phase.[47]

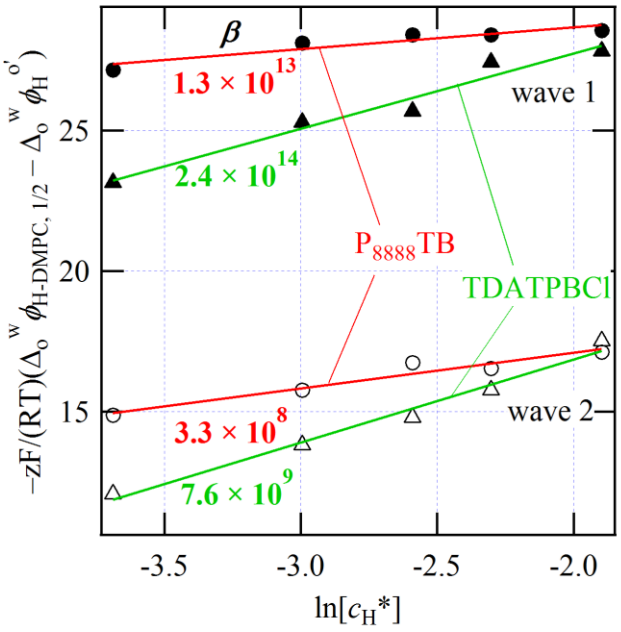

Figure 3: Plots of $-zF/(RT)(\Delta_o^w\phi_{H-DMPC,1/2} - \Delta_o^w\phi_{H^+}^{o'})$ versus $\ln[c_{H^+}^*]$, for Cells 2 or 3 with $P_{8888}TB$ or TDATPBCl as the organic phase supporting electrolyte. $\Delta_o^w\phi_{H-DMPC,1/2}$, $\Delta_o^w\phi_{H^+}^{o'}$, and $c_{H^+}^*$ are the half-wave potential recorded from Figures S4 and S5, the formal proton transfer potential (0.580V – estimated from the value at a w|DCE interface[43]), and the initial proton concentration in the aqueous phase, respectively.

The present system however, exhibits an array of advantages. By using chloroform, appreciable [DMPC] were made possible, thus increasing i_{ss} to observable levels. At the same time, the cell was made conductive by employing a highly dissociative, inert IL as the supporting electrolyte. Most critically, the system employed herein allows for direct thermodynamic assessment of proton-DMPC interaction based on established liquid|liquid mechanisms.[28]

One can also estimate the pK_as of DMPC in $CHCl_3$ for waves 1 and 2 (since, $K_a = 1/\beta$), with $P_{8888}TB$ as the supporting electrolyte (Figure S4 of the SI), as 13.1 and 8.5, respectively. Furthermore, eq. 3 can be rewritten in terms of pK_a:[48,49]

$$\Delta_o^w\phi_{1/2,HL^+} = \Delta_o^w\phi_{H^+}^{o'} - \frac{2.303RT}{mF}pK_{a,CHCl_3} + \frac{2.303RT}{F}pH_w \quad (4)$$

These results agree well with previous studies of ligand assisted ion transfer reactions at liquid|liquid interfaces.[42,48-56]

In order to explore this further, while taking into account the aqueous acid dissociation of H_2SO_4 (pK_a's of –6.62 and 1.99),[57] a simulation was constructed using Comsol Multiphysics software. H_2SO_4 was chosen so as to improve the size of the potential window, while high [H_2SO_4] (pH = 1.6-0.8) were used so that reaction was continuously limited by the diffusion of DMPC; *i.e.* [H^+]>>[DMPC]. Additionally, since H_2SO_4 was both analyte and supporting electrolyte, lower concentrations would elicit additional effects from increased solution resistivity. The TOC/TIC mechanism was incorporated into the simulation (Figure S3 of the SI), while the two-dimensional axial symmetric micropipette geometry employed, along with the generalized theory of facilitated and simple ion transfer, has been described in detail elsewhere.[34,52]

Figure S7A in the SI depicts the simulated CVs obtained a low pH (1.6-0.8) and demonstrates a good agreement with the experimental curves shown in Figure S4. Using eq. 4, the shift in $\Delta_o^w\phi_{1/2,HL^+}$ of the simulated traces was plotted in Figure S7B. By performing linear regression on the resultant trend in $\Delta_o^w\phi_{1/2,HL^+}$, the pK_a's can similarly be calculated from the y-intercept; these were found to be 13.2 and 8.6 for waves 1 and 2, respectively, and agree well with the experimentally determined values. This simulation also provides a physical insight into the interaction of these two diprotic species, H_2SO_4 and DMPC, while providing further evidence for a monoprotic H^+-DMPC interaction at low aqueous pH. It is difficult to compare the experimentally determined pK_a values as there is, to the best of our knowledge, no other

experimental evaluation of such values. A recent molecular dynamics simulation has however proposed that in an hydrophobic environment the pK_a of the phosphate group of DMPC would shift by several units toward values more alkaline than that of methylphosphate (of $pK_a = 2.5$).[58] These calculations were performed at the level of a lipid bilayer and do not compare to our system even though it might explain the observed increased basicity of DMPC in the organic $CHCl_3$ solvent and its facilitated protonation at the w|$CHCl_3$ interface.

The large β for the H-DMPC$^+$ complex suggests that proton transfer in this system proceeds with minimal energetic expense and one can envision DMPC use in biphasic systems such as droplet-based microfluidics or for the generation of solar fuels at a liquid|liquid interface. It is illustrated here through O_2 reduction (Figure 4C and equations S1 in SI), but could operate equivalently through H_2 evolution reactions (equation S2 in SI).[59-61] In either case, protons activate the sacrificial electron donor, *e.g.* $Cp^*_2Fe(II)$, forming a metallocene-hydride that reacts further with dissolved O_2 or H^+. Not only would DMPC facilitate proton transfer, but also support the formation of vesicles/micelles that would decrease interfacial surface tension, while enhancing reaction rates for batch reactors. To demonstrate this utility, shake-flask experiments were performed with $Cp^*_2Fe(II)$ and tetramethylammonium tetraphenylborate (TMATPB) was used as a phase transfer catalyst, forming the weakly coordinating HTPB in acidic conditions, which transfers favourably to the organic phase, as described recently.[60,62] Figures 3A and B show photos of the shake-flasks at time 0 and after 24 h, respectively; all vials contained an organic phase with 5 mM $Cp^*_2Fe(II)$, 10 mM DMPC, and 5 mM $P_{8888}TB$, with vial 1 containing an aqueous phase of 50 mM H_2SO_4 and ~10 mM TMATPB, while vial 2 had no aqueous phase. One can qualitatively assess the green colour change between the vials such that 1>>2.

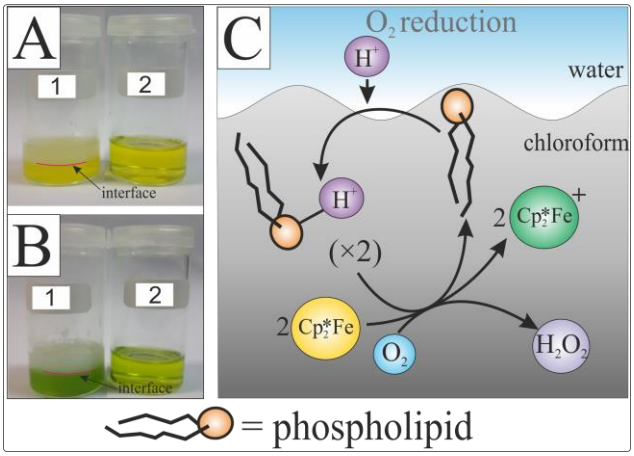

Figure 4: Photographs of shake-flask experiments performed at time 0 (**A**) and after 24 h (**B**) with 5 mM $P_{8888}TB$, 5 mM $Cp^*_2Fe(II)$, and 10 mM DMPC in the organic phase, with (vial 1) or without (vial 2) an aqueous phase containing 150 mM H_2SO_4 and ~10 mM of TMATPB. The interface has been highlighted in pink. **C**: Illustration of O_2 reduction mechanism.

Furthermore, similar conclusions can be drawn from a w|DCE interfacial system with only a catalytic amount of DMPC (~4 µM). Figure 5 shows a similar system, at a w|DCE interface, this time with only ~4 µM of DMPC added to the DCE phase. Vials B1 and B2 both contained an aqueous phase: either with or without acid, respectively. The vibrant green colour in B1 demonstrates that even with such a small amount of DMPC, a significant enhancement in O_2 reduction can be achieved despite using a weak proton phase transfer catalyst such as TMATPB. This is supported by the regeneration of unbound DMPC (Figure 4C). DMPC is unlikely to react with $Cp^*_2Fe(II)$ as it is neither an acid nor an oxidant.

UV/Vis spectra could not be obtained for vials 1, 2, B1, or B2 as the emulsion interfered with the signal measurement.

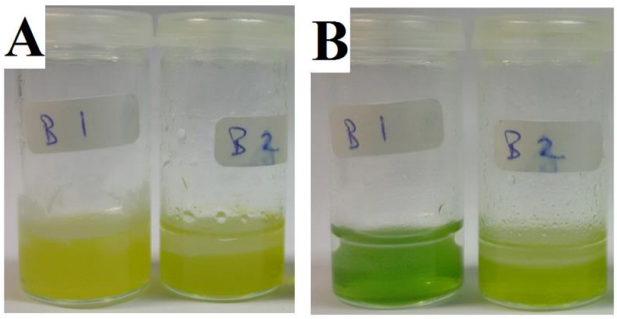

Figure 5: Photographs of shake-flask experiments performed at time 0 (**A**) and after 24 h (**B**) containing 10 mM $Cp^*_2Fe(II)$, ~10 μL of a 1 mM DMPC solution in $CHCl_3$, and 10 mM TDATPBCl in 1,2-dichloroethane; while the aqueous phase contained 10 mM TMATPB, with (vial B1) or without (vial B2) 150 mM H_2SO_4.

CONCLUSIONS

The thermodynamic quantification and mechanistic elucidation of proton-lipid interaction provides a critical insight into the molecular interactions of DMPC towards protons and metal ions using a w|$CHCl_3$ interface. Analysis was made possible by employing an inert IL as supporting electrolyte in the organic phase. In this way, the study highlights the usefulness of ionic liquids as supporting electrolytes, which permit one to work with unusual solvents with low permittivity (*e.g.* $CHCl_3$), which can in turn be useful in the dissolution of particular chemical reagents.

Two 1:1, proton:DMPC stoichiometries with distinct complexation constant values equal to 1.3×10^{13} and 3.3×10^{8} L mol^{-1} were estimated, indicating the independent coordination of protons to two sites on the DMPC molecule (*e.g.* the phosphine oxide and carbonyl moieties). These results provide evidence that DMPC is a powerful vector for Lewis acid (*e.g.* H^+ and Li^+) transfer into organic solutions and they show how it plays crucial roles in biological/biomimetic applications, including chemical communication. This also demonstrates how DMPC can

convert the w|$CHCl_3$ interface from one that repels to one that attracts H^+ and may further illuminate the proton/membrane concentration/surface diffusion phenomena.

Meanwhile, shake-flask experiments illustrate the feasibility of DMPC supported emulsion systems towards solar fuel energy applications based on the liquid|liquid platform. These data have further implications towards micro-emulsions and synthetic reactor systems.

ASSOCIATED CONTENT

Supporting Information. Experimental Details, additional CV Experiments, Comsol simulation of the facilitated ion transfer, shake-flask Experiments.

ACKNOWLEDGMENT

The authors acknowledge support from Labex MICHEM, CNRS, Paris Diderot University, and UPMC.

REFERENCES

(1) Brändén, M.; Sandén, T.; Brzezinski, P.; Widengren, J. Localized proton microcircuits at the biological membrane-water interface *Proc Natl Acad Sci U S A* **2006**, *103*, 19766-19770.

(2) Wolf, Maarten G.; Grubmüller, H.; Groenhof, G. Anomalous Surface Diffusion of Protons on Lipid Membranes *Biophys. J.* **2014**, *107*, 76-87.

(3) van Swaay, D.; deMello, A. Microfluidic methods for forming liposomes *Lab on a Chip* **2013**, *13*, 752-767.

(4) Tomasi, R.; Noel, J.-M.; Zenati, A.; Ristori, S.; Rossi, F.; Cabuil, V.; Kanoufi, F.; Abou-Hassan, A. Chemical communication between liposomes encapsulating a chemical oscillatory reaction *Chem. Sci.* **2014**, *5*, 1854-1859.

(5) Tompkins, N.; Li, N.; Girabawe, C.; Heymann, M.; Ermentrout, G. B.; Epstein, I. R.; Fraden, S. Testing Turing's theory of morphogenesis in chemical cells *Proc. Natl. Acad. Sci. U. S. A.* **2014**, *111*, 4397-4402.

(6) Torbensen, K.; Rossi, F.; Pantani, O. L.; Ristori, S.; Abou-Hassan, A. Interaction of the Belousov–Zhabotinsky Reaction with Phospholipid Engineered Membranes *J. Phys. Chem. B* **2015**, *119*, 10224-10230.

(7) Zhang, J.; Unwin, P. R. Proton Diffusion at Phospholipid Assemblies *J. Am. Chem. Soc.* **2002**, *124*, 2379-2383.

(8) Cannan, S.; Zhang, J.; Grunfeld, F.; Unwin, P. R. Scanning Electrochemical Microscopy (SECM) Studies of Oxygen Transfer across Phospholipid Monolayers under Surface Pressure Control: Comparison of Monolayers at Air/Water and Oil/Water Interfaces *Langmuir* **2004**, *20*, 701-707.

(9) Méndez, M. A.; Nazemi, Z.; Uyanik, I.; Lu, Y.; Girault, H. H. Melittin Adsorption and Lipid Monolayer Disruption at Liquid–Liquid Interfaces *Langmuir* **2011**, *27*, 13918-13924.

(10) Navrátil, T.; Šestáková, I.; Štulík, K.; Mareček, V. Electrochemical Measurements on Supported Phospholipid Bilayers: Preparation, Properties and Ion Transport Using Incorporated Ionophores *Electroanalysis* **2010**, *22*, 2043-2050.

(11) Mareček, V.; Lhotský, A.; Jänchenová, H. Mechanism of Lecithin Adsorption at a Liquid|Liquid Interface *J. Phys. Chem. B* **2003**, *107*, 4573-4578.

(12) Tsionsky, M.; Zhou, J.; Amemiya, S.; Fan, F.-R. F.; Bard, A. J.; Dryfe, R. A. W. Scanning Electrochemical Microscopy. 38. Application of SECM to the Study of Charge Transfer through Bilayer Lipid Membranes *Anal. Chem.* **1999**, *71*, 4300-4305.

(13) Kongsuphol, P.; Fang, K. B.; Ding, Z. Lipid bilayer technologies in ion channel recordings and their potential in drug screening assay *Sensors and Actuators B: Chemical* **2013**, *185*, 530-542.

(14) Kontturi, A.-K.; Kontturi, K.; Murtomäki, L.; Quinn, B.; Cunnane, V. J. Study of ion transfer across phospholipid monolayers adsorbed at micropipette ITIES *J. Electroanal. Chem.* **1997**, *424*, 69-74.

(15) Chowdhury, M.; Kataky, R. Emulsification at the Liquid/Liquid Interface: Effects of Potential, Electrolytes and Surfactants *ChemPhysChem* **2016**, *17*, 105-111.

(16) Herzog, G. Recent developments in electrochemistry at the interface between two immiscible electrolyte solutions for ion sensing *Analyst* **2015**, *140*, 3888-3896.

(17) Samec, Z.; Langmaier, J.; Kakiuchi, T. Charge-transfer processes at the interface between hydrophobic ionic liquid and water *Pure Appl. Chem.* **2009**, *81*, 1473-1488.

(18) Liu, S.; Li, Q.; Shao, Y. Electrochemistry at micro- and nanoscopic liquid/liquid interfaces *Chem. Soc. Rev.* **2011**, *40*, 2236-2253.

(19) Poltorak, L.; Herzog, G.; Walcarius, A. Electrochemically Assisted Generation of Silica Deposits Using a Surfactant Template at Liquid/Liquid Microinterfaces *Langmuir* **2014**, *30*, 11453-11463.

(20) O'Sullivan, S.; Alvarez de Eulate, E.; Yuen, Y. H.; Helmerhorst, E.; Arrigan, D. W. M. Stripping voltammetric detection of insulin at liquid-liquid microinterfaces in the presence of bovine albumin *Analyst* **2013**, *138*, 6192-6196.

(21) Colombo, M. L.; Sweedler, J. V.; Shen, M. Nanopipet-Based Liquid–Liquid Interface Probes for the Electrochemical Detection of Acetylcholine, Tryptamine, and Serotonin via Ionic Transfer *Anal. Chem.* **2015**, 5095-5100.

(22) Hartvig, R. A.; van de Weert, M.; Østergaard, J.; Jorgensen, L.; Jensen, H. Formation of Dielectric Layers and Charge Regulation in Protein Adsorption at Biomimetic Interfaces *Langmuir* **2012**, *28*, 1804-1815.

(23) Sairi, M.; Chen-Tan, N.; Neusser, G.; Kranz, C.; Arrigan, D. W. M. Electrochemical Characterisation of Nanoscale Liquid|Liquid Interfaces Located at Focused Ion Beam-Milled Silicon Nitride Membranes *ChemElectroChem* **2015**, *2*, 98-105.

(24) Kim, J.; Izadyar, A.; Shen, M.; Ishimatsu, R.; Amemiya, S. Ion Permeability of the Nuclear Pore Complex and Ion-Induced Macromolecular Permeation as Studied by Scanning Electrochemical and Fluorescence Microscopy *Anal. Chem.* **2014**, *86*, 2090-2098.

(25) Kim, J.; Izadyar, A.; Nioradze, N.; Amemiya, S. Nanoscale Mechanism of Molecular Transport through the Nuclear Pore Complex As Studied by Scanning Electrochemical Microscopy *J. Am. Chem. Soc.* **2013**, *135*, 2321-2329.

(26) Velický, M.; Tam, K. Y.; Dryfe, R. A. W. Mechanism of Ion Transfer in Supported Liquid Membrane Systems: Electrochemical Control over Membrane Distribution *Anal. Chem.* **2014**, *86*, 435-442.

(27) Stockmann, T. J.; Zhang, J.; Montgomery, A.-M.; Ding, Z. Electrochemical assessment of water|ionic liquid biphasic systems towards cesium extraction from nuclear waste *Anal. Chim. Acta* **2014**, *821*, 41-47.

(28) Reymond, F.; Lagger, G.; Carrupt, P.-A.; Girault, H. H. Facilitated ion transfer reactions across oil|water interfaces. Part II. Use of the convoluted current for the calculation of the association constants and for an amperometric determination of the stoichiometry of MLjz+ complexes *J. Electroanal. Chem.* **1998**, *451*, 59-76.

(29) Diba, F. S.; Lee, H. J. Amperometric sensing of sodium, calcium and potassium in biological fluids using a microhole supported liquid/gel interface *J. Electroanal. Chem.* **2016**, *769*, 5-10.

(30) Wohlfarth, C. In *CRC Handbook of Chemistry and Physics*; CRC Press: Boca Raton, FL, 2011; Vol. 91st, p 6-186.

(31) Ohde, H.; Uehara, A.; Yoshida, Y.; Maeda, K.; Kihara, S. Some factors in the voltammetric measurement of ion transfer at the micro aqueous | organic solution interface *J. Electroanal. Chem.* **2001**, *496*, 110-117.

(32) Olaya, A. J.; Ge, P.; Girault, H. H. Ion transfer across the water|trifluorotoluene interface *Electrochem. Commun.* **2012**, *19*, 101-104.

(33) Toth, P. S.; Dryfe, R. A. W. Novel organic solvents for electrochemistry at the liquid/liquid interface *Analyst* **2015**, *140*, 1947-1954.

(34) Stockmann, T. J.; Ding, Z. Tetraoctylphosphonium Tetrakis(pentafluorophenyl)borate Room Temperature Ionic Liquid toward Enhanced Physicochemical Properties for Electrochemistry *J. Phys. Chem. B* **2012**, *116*, 12826-12834.

(35) Li, R.; Winter, R. E. K.; Kramer, J.; Gokel, G. W. Alkali metal and ammonium cation–arene interactions with tetraphenylborate anion *Supramol. Chem.* **2010**, *22*, 73-80.

(36) Stockmann, T. J.; Ding, Z. Electrochemical behavior of ferrocenes in tributylmethylphosphonium methyl sulfate mixtures with water and 1,2-dichloroethane *Can. J. Chem.* **2015**, *93*, 13-21.

(37) Stockmann, T. J.; Lu, Y.; Zhang, J.; Girault, H. H.; Ding, Z. Interfacial Complexation Reactions of Sr2+ with Octyl(phenyl)-N,N-diisobutylcarbamoylmethylphosphine Oxide for Understanding Its Extraction in Reprocessing Spent Nuclear Fuels *Chem. Eur. J.* **2011**, *17*, 13206-13216.

(38) Rodgers, P. J.; Amemiya, S. Cyclic voltammetry at micropipet electrodes for the study of ion-transfer kinetics at liquid/liquid interfaces *Anal. Chem.* **2007**, *79*, 9276-9285.

(39) Hore, D. K.; Walker, D. S.; MacKinnon, L.; Richmond, G. L. Molecular Structure of the Chloroform−Water and Dichloromethane−Water Interfaces† *J. Phys. Chem. C* **2007**, *111*, 8832-8842.

(40) Moore, F. G.; Richmond, G. L. Integration or Segregation: How Do Molecules Behave at Oil/Water Interfaces? *Acc. Chem. Res.* **2008**, *41*, 739-748.

(41) Zangi, R.; Engberts, J. B. F. N. Physisorption of Hydroxide Ions from Aqueous Solution to a Hydrophobic Surface *J. Am. Chem. Soc.* **2005**, *127*, 2272-2276.

(42) Nestor, U.; Wen, H.; Girma, G.; Mei, Z.; Fei, W.; Yang, Y.; Zhang, C.; Zhan, D. Facilitated Li+ ion transfer across the water/1,2-dichloroethane interface by the solvation effect *Chem. Commun.* **2014**, *50*, 1015-1017.

(43) Olaya, A. J.; Méndez, M. A.; Cortes-Salazar, F.; Girault, H. H. Voltammetric determination of extreme standard Gibbs ion transfer energy *J. Electroanal. Chem.* **2010**, *644*, 60-66.

(44) Ogura, K.; Kihara, S.; Umetani, S.; Matsui, M. Voltammetric study on the transfer of alkali and alkaline earth metal ions at the aqueous/organic interface facilitated by phosphine oxides *Bull. Chem. Soc. Jpn.* **1993**, *66*, 1971-1978.

(45) LeSuer, R. J.; Geiger, W. E. Improved Electrochemistry in Low-Polarity Media Using Tetrakis(pentafluorophenyl)borate Salts as Supporting Electrolytes *Angew. Chem. Int. Ed.* **2000**, *39*, 248-250.

(46) Rosatzin, T.; Bakker, E.; Suzuki, K.; Simon, W. Lipophilic and immobilized anionic additives in solvent polymeric membranes of cation-selective chemical sensors *Anal. Chim. Acta* **1993**, *280*, 197-208.

(47) Holub, K.; Jänchenová, H.; Štulík, K.; Mareček, V. Proton transfer across a liquid/liquid interface facilitated by phospholipid interfacial films *J. Electroanal. Chem.* **2009**, *632*, 8-13.

(48) Su, B.; Li, F.; Partovi-Nia, R.; Gros, C.; Barbe, J. M.; Samec, Z.; Girault, H. H. Evidence of tetraphenylporphyrin monoacids by ion-transfer voltammetry at polarized liquid vertical bar liquid interfaces *Chem. Commun.* **2008**, 5037-5038.

(49) Matsuda, H.; Yamada, Y.; Kanamori, K.; Kudo, Y.; Takeda, Y. Facilitation effect of neutral macrocyclic ligands on the ion transfer across the interface between aqueous and organic solutions. I. Theoretical equation of ion-transfer-polarographic current-potential curves and its experimental verification *Bull. Chem. Soc. Jpn.* **1991**, *64*, 1497-1508.

(50) Bakker, E. Electroanalysis with Membrane Electrodes and Liquid–Liquid Interfaces *Anal. Chem.* **2016**, *88*, 395-413.

(51) Dassie, S. A. Facilitated proton transfer or protonated species transfer reactions across oil|water interfaces *J. Electroanal. Chem.* **2014**, *728*, 51-59.

(52) Nishi, N.; Murakami, H.; Imakura, S.; Kakiuchi, T. Facilitated transfer of alkali-metal cations by dibenzo-18-crown-6 across the electrochemically polarized interface between an aqueous solution and a hydrophobic room-temperature ionic liquid *Anal. Chem.* **2006**, *78*, 5805-5812.

(53) Langmaier, J.; Samec, Z. Voltammetry of Ion Transfer across a Polarized Room-Temperature Ionic Liquid Membrane Facilitated by Valinomycin: Theoretical Aspects and Application *Anal. Chem.* **2009**, *81*, 6382-6389.

(54) Kudo, Y.; Katsuta, S.; Takeda, Y. Evaluation of overall extraction constants for the crown ether-complex ions of alkali and alkaline-earth metal with counter picrate ions from water into nitrobenzene based on their component equilibrium constants *J. Mol. Liq.* **2012**, *173*, 66-70.

(55) Meng, X.; Liang, Z.; Li, B.; Xu, X.; Li, Q.; Zhao, W.; Xie, S.; Shao, Y. Investigation of transfer behavior of protonated pyridine at the liquid/liquid interface using dual micropipettes *J. Electroanal. Chem.* **2011**, *656*, 125-129.

(56) Cui, R. F.; Li, Q.; Gross, D. E.; Meng, X.; Li, B.; Marquez, M.; Yang, R. H.; Sessler, J. L.; Shao, Y. H. Anion Transfer at a Micro-Water/1,2-Dichloroethane Interface Facilitated by beta-Octafluoro-meso-octamethylcalix 4 pyrrole *J. Am. Chem. Soc.* **2008**, *130*, 14364-14365.

(57) Haynes, W. M. In *CRC Handbook of Chemistry and Physics*; CRC Press/Taylor: Boca Raton, FL, 2013; Vol. 94, p 5.92.

(58) Teixeira, V. H.; Vila-Viçosa, D.; Baptista, A. M.; Machuqueiro, M. Protonation of DMPC in a Bilayer Environment Using a Linear Response Approximation *J. Chem. Theory Comput.* **2014**, *10*, 2176-2184.

(59) Smirnov, E.; Scanlon, M. D.; Momotenko, D.; Vrubel, H.; Méndez, M. A.; Brevet, P.-F.; Girault, H. H. Gold Metal Liquid-Like Droplets *ACS Nano* **2014**, *8*, 9471-9481.

(60) Rivier, L.; Stockmann, T. J.; Méndez, M. A.; Scanlon, M. D.; Peljo, P.; Opallo, M.; Girault, H. H. Decamethylruthenocene Hydride and Hydrogen Formation at Liquid|Liquid Interfaces *J. Phys. Chem. C* **2015**, *119*, 25761-25769.

(61) Su, B.; Nia, R. P.; Li, F.; Hojeij, M.; Prudent, M.; Corminboeuf, C.; Samec, Z.; Girault, H. H. H2O2 generation by decamethylferrocene at a liquid vertical bar liquid interface *Angew. Chem. Int. Ed.* **2008**, *47*, 4675-4678.

(62) Ge, P.; Todorova, T. K.; Patir, I. H.; Olaya, A. J.; Vrubel, H.; Mendez, M.; Hu, X.; Corminboeuf, C.; Girault, H. H. Biphasic water splitting by osmocene *Proc. Natl. Acad. Sci* **2012**, *109*, 11558-11563.

TOC GRAPHICS